Two-photon process of a single two-level atom simultaneously absorbing or emitting two photons distributed in different cavities and its applications

Tong Liu [1,*] Jin Xu [2] Qi-Ping Su [3,†] Yan-Hui Zhou [1] and Qi-Cheng Wu [1]

[1] *Quantum Information Research Center, Shangrao Normal University, Shangrao 334001, China*

[2] *School of Physics and Electronic Information, Shangrao Normal University, Shangrao 334001, China*

[3] *Department of Physics, Hangzhou Normal University, Hangzhou 311121, China*

(Received 25 November 2021; accepted 20 December 2022; published 28 December 2022)

We propose an approach for achieving a two-photon process in which a *single two-level* atom can simultaneously absorb or emit *two photons* separately distributed in two cavities. This two-photon process is realized by a two-level atom dispersively coupled to a classical pulse and two cavities. The main advantage of this proposal lies in the fact that because only two levels of the atom are used, i.e., no auxiliary atomic levels are utilized, decoherence from the higher energy levels of the atom is avoided. In addition, we find that the two-photon process can enable the synthesis of a hybrid atom-cavity-cavity Greenberger-Horne-Zeilinger (GHZ) entangled state. As an example, we further discuss the experimental feasibility of creating the proposed hybrid GHZ state in a circuit QED system. This proposal is quite general and can be implemented in a wide range of physical systems, such as a natural or artificial atom coupled to two optical or microwave cavities.

DOI: 10.1103/PhysRevA.106.063721

I. INTRODUCTION

The two-photon process was predicted by Göppert-Mayer in 1931 [1] and since then has drawn much attention in the realms of quantum information processing and quantum communication. The two-photon process plays a vital role in fluorescent imaging [2], quantum light sources [3], microfabrication [4], etc. The two-photon maser oscillator has been experimentally realized using a three-level atom [5]. In the past few decades, a number of schemes have been proposed for realizing the two-photon process [6–9]. For example, Refs. [6,7] proposed that two-photon stimulated emission and absorption can be obtained via a *multilevel* atom, which interacts with a two-mode field through the adiabatic elimination of the atomic auxiliary levels. In Refs. [6,7], the cavity frequency is equal to the sum of the transition frequencies of the two atoms. References [8,9] found that through a *three-level* atom interacting with two quantized cavity modes, one can obtain the effective two-photon coupling between the atom and the cavity modes. On the other hand, one single photon or atom simultaneously exciting two atoms has been widely studied recently [10–15]. For instance, Ref. [10] showed that two atoms can jointly absorb one photon if the two atoms are coupled to a cavity in the ultrastrong-coupling regime. In this proposal, the cavity frequency is equal to the sum of the transition frequencies of the two atoms. References [11,12] found that a single photon can simultaneously excite two atoms without ultrastrong coupling. Moreover, Refs. [13] and [14] proposed that a single atom can simultaneously excite two atoms with and without ultrastrong coupling. Recently, Ref. [15] reported the experimental observation of simultaneous excitation of two atoms by a pair of photons in a superconducting circuit.

Greenberger-Horne-Zeilinger (GHZ) entangled states play a central role in error correction [16], quantum teleportation [17], quantum metrology [18], quantum communication [19], entanglement swapping [20], etc. Moreover, GHZ states can be applied to violate the Bell inequality [21]. In recent years, a large number of theoretical proposals have been made for preparing GHZ states in various physical systems [22–34]. Experimentally, the creation of GHZ states with 3 nitrogen-vacancy (NV) center spins [35], 12–18 photonic qubits [36,37], 14 ionic qubits [38], 20 atomic qubits [39], and 3–20 superconducting qubits [40–43] has been reported.

In this paper we present an approach for realizing a two-photon process in which a *single two-level* atom can simultaneously absorb or emit *two photons*, which are separately distributed in two cavities. This two-photon process is realized by a two-level atom dispersively coupled to a classical pulse and two cavities. Since no auxiliary atomic levels are used in our proposal, decoherence from higher energy levels of the atom is avoided.

The regular two-photon process has shown that an atom coupled to a single cavity can absorb and emit two photons in one cavity mode. Different from the regular two-photon process, in our proposal, the two photons are separately distributed in two cavity modes. We stress that this work differs from the previous works [6–9]. In our work, the two-photon process is realized by using only a *two-level* atom, while Refs. [6–9] employed a *multilevel* atom to implement a two-photon process. The present work is also different from the previous works [10–15], which focus on a different topic, i.e., one single photon or atom simultaneously exciting two atoms. In this work, we find that the two-photon process can allow the

*liutong7500755@163.com

†sqp@hznu.edu.cn

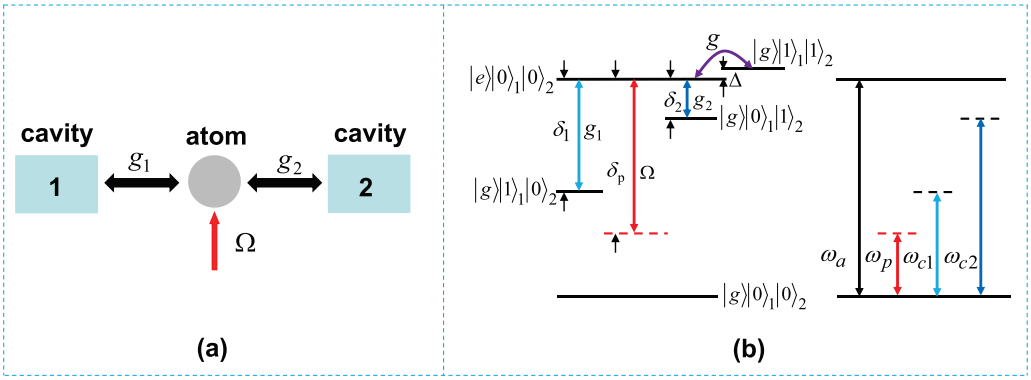

FIG. 1. (a) Diagram of the setup for two cavities (1 and 2) coupled to an atom. Here, the atom can be a natural atom or a solid-state artificial atom (e.g., superconducting qubit, NV center, quantum dot, etc.) which is coupled to two optical or microwave cavities. (b) Schematic diagram of the energy levels of the whole system. Cavities 1 and 2 are coupled to the atom with coupling strengths g_1 and g_2 and detunings δ_1 and δ_2, respectively. In addition, a classical pulse is applied to the atom with Rabi frequency Ω and detuning δ_p. Here, ω_a, ω_p, ω_{c1}, and ω_{c2} are the frequencies of the atom, the pulse, cavity 1, and cavity 2, respectively. In numerical simulations of Figs. 3 and 4(a), we choose $\delta_1 = 72g_2$, $\delta_2 = 36g_2$, and $\delta_p = 109.432g_2$. Thus, we have $\omega_{c1} = \omega_a - 36g_2$, $\omega_{c2} = \omega_a - 72g_2$, and $\omega_p = \omega_a - 109.342g_2$.

generation of an atom-cavity-cavity (three-body) hybrid GHZ state. As an example, we further investigate the experimental feasibility of creating the hybrid GHZ state in a circuit QED system. This proposal is quite general and can be applied to a wide range of physical systems, such as a natural atom or a solid-state artificial atom (e.g., superconducting qubit, NV center, quantum dot, etc.) coupled to two optical or microwave cavities.

This paper is organized as follows. Section II introduces a method for realizing a two-photon process, in which a single two-level atom simultaneously absorbs or emits two photons distributed in two cavities. Section III shows that the two-photon process can be used to create a hybrid atom-cavity-cavity GHZ state. Section IV investigates the experimental feasibility of creating the hybrid GHZ in a circuit QED system. A brief concluding summary is given in Sec. V.

II. TWO-PHOTON PROCESS WITH A TWO-LEVEL ATOM SIMULTANEOUSLY ABSORBING OR EMITTING TWO PHOTONS

Consider a system consisting of two cavities (1 and 2) and a single two-level atom (i.e., a qubit) with the ground state $|g\rangle$ and the excited state $|e\rangle$, as shown in Fig. 1. Assume that cavities 1 and 2 are coupled to the atom with coupling strengths g_1 and g_2 as well as detunings $\delta_1 = \omega_a - \omega_{c1} > 0$ and $\delta_2 = \omega_a - \omega_{c2} > 0$, respectively. Moreover, a classical pulse is applied to the atom with Rabi frequency Ω and detuning $\delta_p = \omega_a - \omega_p > 0$. Here, ω_{c1} and ω_{c2} are, respectively, the frequencies of cavities 1 and 2, ω_a is the transition frequency of the atom, and ω_p is the frequency of the pulse.

In the interaction picture, after making the rotating-wave approximation (RWA), the Hamiltonian of the whole system can be described as (in units of $\hbar = 1$)

$$\begin{aligned} H_I = {} & g_1(\hat{a}_1\sigma^+ e^{i\delta_1 t} + \hat{a}_1^\dagger\sigma^- e^{-i\delta_1 t}) \\ & + g_2(\hat{a}_2\sigma^+ e^{i\delta_2 t} + \hat{a}_2^\dagger\sigma^- e^{-i\delta_2 t}) \\ & + \Omega(\sigma^+ e^{i\delta_p t} + \sigma^- e^{-i\delta_p t}), \end{aligned} \tag{1}$$

where $\sigma^+ = |e\rangle\langle g|$ and $\sigma^- = |g\rangle\langle e|$ are, respectively, the raising and lowering operators of the atom and $\hat{a}_1$ and $\hat{a}_1^\dagger$ ($\hat{a}_2$ and $\hat{a}_2^\dagger$) are, respectively, the photon annihilation and creation operators for cavity 1 (2).

By using James's effective Hamiltonian method [44,45], one can obtain the effective Hamiltonian

$$H_{\rm eff}(t) = H_{\rm eff}^{(2)}(t) + H_{\rm eff}^{(3)}(t) + \cdots + H_{\rm eff}^{(n)}(t), \tag{2}$$

where $H_{\rm eff}^{(2)}(t)$, $H_{\rm eff}^{(3)}(t)$, and $H_{\rm eff}^{(n)}(t)$ are second-order, third-order, and nth-order effective Hamiltonians, respectively. Our proposal aims to realize a tripartite interaction for a two-photon process involving two operators, $\sigma^-\hat{a}_1^\dagger\hat{a}_2^\dagger$ and $\sigma^+\hat{a}_1\hat{a}_2$. When the Hilbert space is expanded in the basis states $|e\rangle|n_1\rangle_1|n_2\rangle_2$ and $|g\rangle|n_1+1\rangle_1|n_2+1\rangle_2$, the effective Hamiltonian can be expanded up to third order, while higher-order terms are neglected. Here, $|n_1\rangle_1$ and $|n_2\rangle_2$ are, respectively, the Fock states of cavities 1 and 2.

We focus on the third-order term and neglect the higher-order terms. Thus, under the large detuning conditions $\delta_1 \gg g_1, \delta_2 \gg g_2, \delta_p \gg \Omega$, the second-order and third-order effective Hamiltonians are given by [44,45]

$$H_{\rm eff}^{(2)} = \frac{1}{i}H_I(t)\int^t H_I(t')dt', \tag{3}$$

$$H_{\rm eff}^{(3)} = -H_I(t)\int^t H_I(t_1)\int^{t_1} H_I(t_2)dt_2dt_1. \tag{4}$$

Substituting Hamiltonian H_I [i.e., Eq. (1)] into formula (3) and dropping fast oscillating terms using the RWA, one can obtain the second-order effective Hamiltonian (see Appendix A) [44–48]

$$H_{\rm eff}^{(2)} = \left[\lambda_1\left(\hat{a}_1^\dagger\hat{a}_1 + \tfrac{1}{2}\right) + \lambda_2\left(\hat{a}_2^\dagger\hat{a}_2 + \tfrac{1}{2}\right) + \lambda_p\right]\sigma_z, \tag{5}$$

where $\lambda_1 = \frac{g_1^2}{\delta_1}$, $\lambda_2 = \frac{g_2^2}{\delta_2}$, $\lambda_p = \frac{\Omega^2}{\delta_p}$, and $\sigma_z = |e\rangle\langle e| - |g\rangle\langle g|$.

Then we consider the third-order case by employing James's effective Hamiltonian method [45]. Assuming that $\delta_p \gg \delta_1 > \delta_2$ and satisfying $\delta_p \gtrsim \delta_1 + \delta_2$, $H_{\rm eff}^{(3)}$ can be approximated as the following form using the RWA (a detailed

derivation of $H_{\rm eff}^{(3)}$ is shown in Appendix B) [44–48]:

$$H_{\rm eff}^{(3)} = -g(\sigma^- \hat{a}_1^\dagger \hat{a}_2^\dagger e^{i\Delta t} + \sigma^+ \hat{a}_1 \hat{a}_2 e^{-i\Delta t}), \tag{6}$$

where $g = g_1 g_2 \Omega[\frac{1}{\delta_2(\delta_p-\delta_2)} + \frac{1}{\delta_1(\delta_p-\delta_1)}]$ is the effective coupling strength, $\Delta = \delta_p - \delta_1 - \delta_2$. Accordingly, one can obtain the effective Hamiltonian

$$H_{\rm eff} = H_{\rm eff}^{(2)} + H_{\rm eff}^{(3)} = H_0 + H_{\rm int}, \tag{7}$$

with

$$H_0 = \left[\lambda_1\left(\hat{a}_1^\dagger \hat{a}_1 + \tfrac{1}{2}\right) + \lambda_2\left(\hat{a}_2^\dagger \hat{a}_2 + \tfrac{1}{2}\right) + \lambda_p\right]\sigma_z, \tag{8}$$

$$H_{\rm int} = -g(\sigma^- \hat{a}_1^\dagger \hat{a}_2^\dagger e^{i\Delta t} + \sigma^+ \hat{a}_1 \hat{a}_2 e^{-i\Delta t}). \tag{9}$$

From the Hamiltonian $H_{\rm int}$, one can see that the atom is coupled to cavities 1 and 2 simultaneously. The operator $\sigma^- \hat{a}_1^\dagger \hat{a}_2^\dagger$, involved in the Hamiltonian $H_{\rm int}$, represents a tripartite interaction for a two-photon process, in which the atom makes the transition from its upper level $|e\rangle$ to lower level $|g\rangle$, which is accompanied by the emission of two photons into cavities 1 and 2, respectively; however, the operator $\sigma^+ \hat{a}_1 \hat{a}_2$ represents a tripartite interaction for a reverse two-photon process, in which the atom makes the transition $|g\rangle \to |e\rangle$, which is accompanied by the absorption of two photons which are originally in cavities 1 and 2, respectively.

We note that the previous works considered a single two-level atom coupled to two cavity modes and two strong classical pulses [49] or a strong classical pulse [50], which employed the strong-driving limit or large detuning in the derivation of the effective Hamiltonian. In this sense, they are related to this work. However, Refs. [49,50] are different from our work. References [49,50] focused on how to construct the effective interaction Hamiltonians between two cavities, where the degree of freedom for the atom was omitted by choosing the atomic initial state. However, we concentrated on how to derive an atom-cavity-cavity tripartite-interaction effective Hamiltonian for simultaneously coupling two cavities and an atom. Thus, the form of our effective Hamiltonian is different from that in Refs. [49,50].

III. GENERATION OF A HYBRID GHZ ENTANGLED STATE

Now we show that the two-photon process, described by the effective Hamiltonian (7), can be used to generate a hybrid atom-cavity-cavity GHZ entangled state.

The bare states of the atom-cavity-cavity system can be described as $|e\rangle|n_1\rangle_1|n_2\rangle_2$ and $|g\rangle|n_1+1\rangle_1|n_2+1\rangle_2$. In these bare states, the effective Hamiltonian (7) can be described as

$$H_{e2} = \begin{bmatrix} -(A+\lambda_1+\lambda_2) & -g_e e^{i\Delta t} \\ -g_e e^{-i\Delta t} & A \end{bmatrix}, \tag{10}$$

where $A = \lambda_1(n_1+1/2) + \lambda_2(n_2+1/2) + \lambda_p$ and $g_e = g\sqrt{(n_1+1)(n_2+1)}$. Here, n_1 and n_2 are the photon numbers of cavities 1 and 2, respectively.

Applying a unitary transformation $U_1 = e^{-iH_0 t}$ to the Hamiltonian (9), one has

$$\begin{aligned} H'_{e2} &= e^{iH_0 t} H_{\rm int} e^{-iH_0 t} \\ &= -g[e^{i\Delta t} e^{-i(\hat{N}+\lambda_p)t} \sigma_{eg}^- \hat{a}_1^\dagger \hat{a}_2^\dagger e^{-i(\hat{N}+\lambda_1+\lambda_2+\lambda_p)t} + \text{H.c.}], \end{aligned} \tag{11}$$

where $\hat{N} = \lambda_1 \hat{a}_1^\dagger \hat{a}_1 + \lambda_2 \hat{a}_2^\dagger \hat{a}_2$. In the bare states $|e\rangle|n_1\rangle_1|n_2\rangle_2$ and $|g\rangle|n_1+1\rangle_1|n_2+1\rangle_2$, the effective Hamiltonian (11) can be described as

$$H'_{e2} = \begin{bmatrix} 0 & -g_e e^{i(\Delta-2A-\lambda_1-\lambda_2)t} \\ -g_e e^{-i(\Delta-2A-\lambda_1-\lambda_2)t} & 0 \end{bmatrix}. \tag{12}$$

Under the Hamiltonian (12), the time evolution of the state $|e\rangle|n_1\rangle_1|n_2\rangle_2$ can be described as

$$\begin{aligned} |e\rangle|n\rangle_1|n\rangle_2 \to \cos[(n+1)gt]|e\rangle|n\rangle_1|n\rangle_2 \\ + i\sin[(n+1)gt]|g\rangle|n+1\rangle_1|n+1\rangle_2, \end{aligned} \tag{13}$$

where we have set $n_1 = n_2 = n$ and $\Delta = 2A + \lambda_1 + \lambda_2$. Accordingly, one can obtain the following relationship between the parameters:

$$\Omega = \sqrt{\frac{\delta_p}{2}[\Delta - 2(n+1)(\lambda_1+\lambda_2)]}. \tag{14}$$

We assume that the atom is in state $|e\rangle$. This can be achieved by applying a classical π pulse resonant to the atom which is initially in state $|g\rangle$. If cavities 1 and 2 are in the vacuum state $|0\rangle_1|0\rangle_2$, the initial state of the whole system is $|e\rangle|0\rangle_1|0\rangle_2$. According to Eq. (13), one can realize a transition $|e\rangle|0\rangle_1|0\rangle_2 \to i|g\rangle|1\rangle_1|1\rangle_2$ for the evolution time $t = \pi/|2g|$. This means that the simultaneous emission of *two* photons into one cavity each is realized by using only a *two-level* atom. If we suppose that the initial state of the whole system is $\frac{1}{\sqrt{2}}(|g\rangle + |e\rangle)|0\rangle_1|0\rangle_2$, we can transfer the state of the atom into a two-cavity entangled state for evolution time $t = \pi/|2g|$, i.e., $\frac{1}{\sqrt{2}}(|g\rangle + |e\rangle)|0\rangle_1|0\rangle_2 \to \frac{1}{\sqrt{2}}|g\rangle(|0\rangle_1|0\rangle_2 + i|1\rangle_1|1\rangle_2)$, which may have a potential application in the error correction [13]. Equation (13) shows that after evolution time $t = \pi/|4g|$, we can generate a hybrid atom-cavity-cavity (three-body) GHZ entangled state

$$|\psi\rangle = \frac{1}{\sqrt{2}}(|e\rangle|0\rangle_1|0\rangle_2 + i|g\rangle|1\rangle_1|1\rangle_2). \tag{15}$$

We should mention that setting $\Delta = 2A + \lambda_1 + \lambda_2$ is absolutely crucial for preparation of the GHZ state. Having a nonzero value for $\Delta - 2A - \lambda_1 - \lambda_2$ results in a detuning between the $|e\rangle|0\rangle_1|0\rangle_2$ and $|g\rangle|1\rangle_1|1\rangle_2$ states, which limits the efficiency of transferring excitations between the atom and the cavity modes. This means that (i) the scheme is sensitive to any imperfections in canceling the two terms [making the precise value of the Rabi frequency in Eq. (14) extremely important] and (ii) the scheme can work only when each cavity starts with a definite Fock state (and not a general superposition).

IV. EXPERIMENTAL FEASIBILITY

In this section, we investigate the experimental feasibility of preparing the proposed hybrid GHZ state in a circuit quantum electrodynamics (QED) system by applying the present proposal. Circuit QED, consisting of superconducting artificial atoms (e.g., flux qubits, charge qubits, phase qubits, and transmon qubits) and superconducting microwave cavities, has become one of the best platforms for achieving quantum computing and quantum information processing [51–58]. Superconducting qubits based on Josephson tunnel junctions

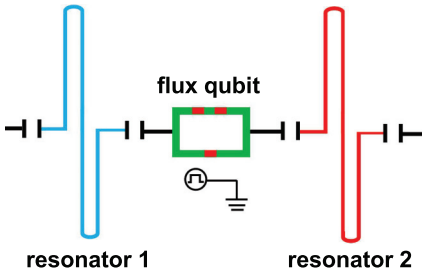

FIG. 2. Diagram of the setup for two superconducting one-dimensional transmission line resonators (1 and 2) coupled to a flux qubit via capacitors.

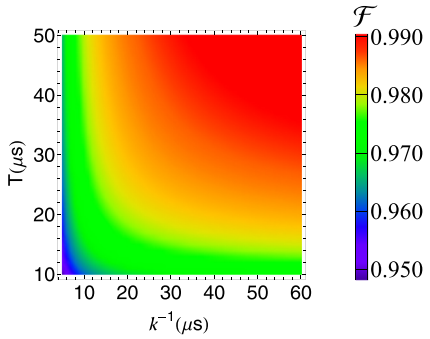

FIG. 3. Fidelity $\mathcal{F}$ versus κ^{-1} and T for the hybrid GHZ entangled state. The values of the parameters used in the numerical simulations are $\kappa_1^{-1} = \kappa^{-1}$, $\kappa_2^{-1} = 1.2\kappa^{-1}$, $\gamma_\varphi^{-1} = T$, and $\gamma^{-1} = 2T$.

have multiple energy levels, and their level spacings can be rapidly adjusted by varying the external control parameters (e.g., changing the magnetic field threading the loop of superconducting qubits) [55–57].

Based on circuit QED, a number of theoretical methods have been proposed for transferring quantum states [59–65], synthesizing entangled states (e.g., GHZ states, W states, and cluster states) [22–31,66–71], and implementing multiqubit quantum gates [72–78] with superconducting qubits or superconducting cavities. In experiments, quantum state transfer between superconducting qubits has been demonstrated [79–81], entangled states with 3–20 superconducting qubits have been generated [40–43], and states of photons (e.g., Fock states, NOON states, two-mode cat states, and Schrödinger-cat states) have been created [82–85]. Recently, high-fidelity two-qubit gates of superconducting qubits have been experimentally implemented in circuit QED [86,87].

Our system consists of two superconducting cavities and a superconducting flux qubit (Fig. 2). As shown in Fig. 2, the two superconducting cavities are one-dimensional transmission line resonators. After taking into account the qubit decoherence and the cavity decay, the dynamics of the lossy system is determined by the Markovian master equation

$$\frac{d\rho}{dt} = -i[H_I, \rho] + \kappa_1\mathcal{L}[\hat{a}_1] + \kappa_2\mathcal{L}[\hat{a}_2] + \gamma\mathcal{L}[\sigma^-] + \gamma_\varphi\mathcal{L}[\sigma_{ee}], \tag{16}$$

where ρ is the density operator of the system, H_I is given by Eq. (1), $\mathcal{L}[\Lambda] = \Lambda\rho\Lambda^+ - \Lambda^+\Lambda\rho/2 - \rho\Lambda^+\Lambda/2$ (with $\Lambda = \hat{a}_1,\ \hat{a}_2,\ \sigma^-,\ \sigma_{ee}$), and $\sigma_{ee} = |e\rangle\langle e|$. In addition, κ_1 and κ_2 are the decay rates of cavities 1 and 2, and γ and γ_φ are the energy relaxation rate and the dephasing rate of the flux qubit.

The fidelity is evaluated by $\mathcal{F} = \sqrt{\langle\psi_{\rm id}|\rho|\psi_{\rm id}\rangle}$, where $|\psi_{\rm id}\rangle$ is the ideal target state (i.e., without decoherence and dissipation considered). Recently, Ref. [88] gave a simple formula for the fidelity reduction of any desired quantum operation.

We numerically calculate the fidelity for the hybrid atom-cavity-cavity GHZ state generation by solving the master equation (16). Numerical calculations are coded in PYTHON by using the QUTIP library [89,90]. The ideal target state $|\psi_{\rm id}\rangle$ is given by Eq. (15), and the initial state of the whole system is given by $|e\rangle|0\rangle_1|0\rangle_2$. In our numerical simulation, we choose $g_1/2\pi = 100$ MHz, $g_2/2\pi = 50$ MHz, $\delta_1/2\pi = 3.66$ GHz, $\delta_2/2\pi = 1.80$ GHz, and $\delta_p/2\pi = 5.4716$ GHz. Thus, according to Eq. (14), we have $\Omega/2\pi \approx 95.84$ MHz, which is available in experiments [91,92]. The coupling strengths here are available because the coupling strength ~636 MHz between a superconducting cavity and a flux qubit was reported in experiments [93].

Figure 3 shows the calculated fidelities as a function of κ^{-1} and T. We find that for $\kappa^{-1} \geqslant 5$ μs and $T \geqslant 10$ μs, the fidelity exceeds 94.82%. When $\kappa^{-1} = 50$ μs and $T = 50$ μs, the fidelity is approximately 98.99%. For $T = 50$ μs, the decoherence times of the flux qubit are 50−100 μs, which is a rather conservative case because a decoherence time of 70 μs to 1 ms for the flux qubit was experimentally reported [94,95]. With the parameters chosen above, the entire operation time is estimated to be 0.86 μs, which is shorter than the decoherence times of the flux qubit used in the numerical simulations. The frequency of a flux qubit is typically within the range of 1–30 GHz. Thus, we choose $\omega_a/2\pi = 6.5$ GHz. According to the qubit-cavity detunings chosen above, we have cavity frequencies $\omega_{c1}/2\pi = 2.84$ GHz and $\omega_{c2}/2\pi = 4.70$ GHz. For cavity decay time $\kappa^{-1} = 50$ μs, the quality factors of cavities 1 and 2 are $Q_1 \sim 8.91 \times 10^5$ and $Q_2 \sim 1.77 \times 10^6$, which are available in experiments [96,97]. A numerical simulation shows that the high-fidelity generation of the hybrid atom-cavity-cavity GHZ state can be achieved by using current circuit QED technology. We now numerically calculate the dynamics of the fidelity, the qubit mean excitation number, and the cavity photon number by solving the master equation (16). The ideal target state $|\psi_{\rm id}\rangle$ of the system is $i|g\rangle|1\rangle_1|1\rangle_2$, and the initial state is $|e\rangle|0\rangle_1|0\rangle_2$. Figure 4 displays the time evolution of the fidelity, the qubit mean excitation number $\langle\sigma^+\sigma^-\rangle$, and the cavity 1 (2) mean photon number $\langle\hat{a}_1^\dagger\hat{a}_1\rangle$ ($\langle\hat{a}_2^\dagger\hat{a}_2\rangle$) as a function of $2gt$. From Fig. 4(a), we can see that the fidelity is approximately 96.93% for $2gt = \pi$. Figure 4(a) shows the reversible excitation exchange between the cavities and the qubit. When $2gt = \pi$, the cavity populations reach a maximum value at around 0.977, while the qubit population reaches its minimum value at around 0.141, which is higher than the initial population in the system.

We can increase the detunings to reduce the minimum value of the qubit population. Figure 4(b) differs from Fig. 4(a) in that it includes the time evolution of the fidelity and the qubit mean excitation number without considering the systematic dissipation (i.e., $\kappa^{-1} = 0$ and $T = 0$). In ad-

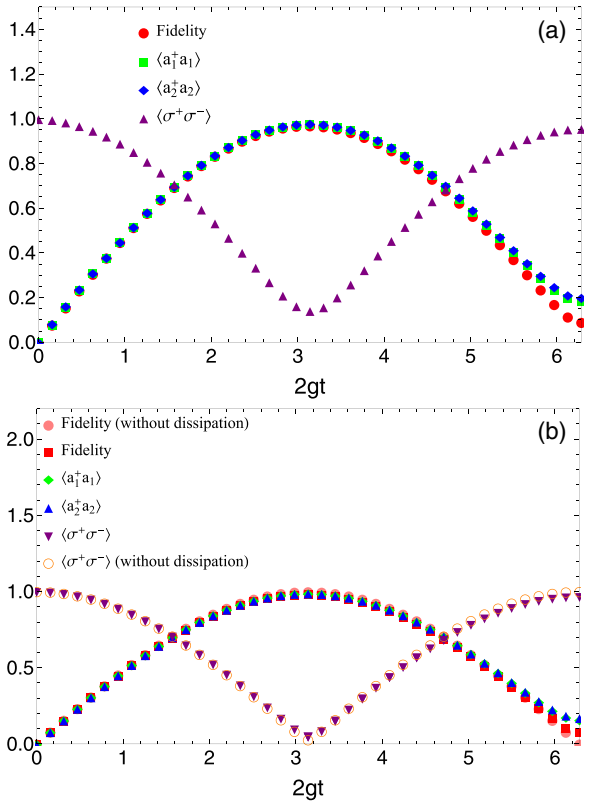

FIG. 4. (a) Time evolution of the fidelity, the qubit mean excitation number, and the mean cavity photon number by taking the systematic dissipation into account. Here, we choose $\kappa^{-1} = 50$ μs and $T = 50$ μs. The other parameters used in the numerical simulation are the same as those used in Fig. 3. (b) Time evolution of the fidelity, the qubit mean excitation number, and the mean cavity photon number while considering the systematic dissipation in (a) but including the time evolution of the fidelity and the qubit mean excitation number without considering the systematic dissipation. Here, we choose $\delta_1/2\pi = 380g_2$, $\delta_2/2\pi = 140g_2$, $\delta_p/2\pi \approx 520.059g_2$, $\kappa^{-1} = 1000$ μs, and $T = 1000$ μs.

dition, we choose $\delta_1/2\pi = 380g_2$, $\delta_2/2\pi = 140g_2$, $\delta_p/2\pi \approx 520.059g_2$, $\kappa^{-1} = 1000$ μs, and $T = 1000$ μs, which are also different from Fig. 4(a). Figure 4(b) shows the optimal fidelities can reach 98.37% (with dissipation) and 99.96% (without dissipation). We observe that for $2gt = \pi$ in Fig. 4(b), the qubit population reaches a minimum value of ∼0.051 (with dissipation) or 0.028 (without dissipation). This population can further decrease when the detunings increase. However, we require longer dissipation times κ^{-1} and T in the numerical simulation because the operation time increases with the increase of the detunings, which may pose a challenge in experiments. In this case, the operation time can be decreased by increasing the coupling strengths. A numerical simulation indicates that the simultaneous emission of two photons into one cavity each is achieved by using a qubit.

The results shown in Fig. 4 are based on the full Hamiltonian H_I [i.e., Eq. (1)]. We now numerically calculate the dynamics of the qubit mean excitation number and the cavity photon number based on the effective Hamiltonian (7) in Fig. 4(a). We find that for $2gt = \pi$ in Fig. 4(a), the photon population (not shown) can reach a maximum value of ∼0.985 (with dissipation) or 0.999 (without dissipation), while the qubit population (not shown) reaches a minimum value of ∼0.065 (with dissipation) or 9.17×10^{-6} (without dissipation). We can see that compared to the case with the populations being transferred based on the full Hamiltonian (1), the excitation of the qubit is fully transferred to cavities 1 and 2. This occurs because the effective Hamiltonian (7) preserves the operator $|e\rangle\langle e| + \hat{a}_1^\dagger \hat{a}_1$ (and, equally, the operator $|e\rangle\langle e| + \hat{a}_2^\dagger \hat{a}_2$); thus, the Hamiltonian H_0 preserves the number of excitations, and $H_{\rm int}$ converts each qubit excitation into one photon in each of the cavity modes and vice versa. In addition, dissipation processes keep the number of excitations constant (dephasing) or reduce it (relaxation). However, the full Hamiltonian (1) does not preserve the number of excitations the way the effective Hamiltonian does; thus, the significant population (i.e., the cavity-qubit population is much higher than the system's initial population) of Fig. 4(a) (based on the full Hamiltonian) is caused by the limited validity of the effective Hamiltonian. From Fig. 4(b) (based on the full Hamiltonian), we can see that the significant population of Fig. 4(a) can be decreased by increasing the detunings.

V. CONCLUSION

We have presented a method for realizing a two-photon process in which a two-level atom can simultaneously absorb or emit *two photons* separately distributed in two cavities. As shown above, the distinguishing feature of this method is that only two levels of the atom are needed; that is, no auxiliary atomic levels are required. Hence, decoherence from the higher energy levels of the atom is avoided. We have shown that the two-photon process can be used to generate a hybrid atom-cavity-cavity GHZ entangled state. Our numerical simulations demonstrated that within the present circuit QED technology, a hybrid atom-cavity-cavity GHZ state can be created with high fidelity. Finally, this proposal is quite general and can be applied to a wide range of physical systems, such as a natural atom or a solid-state artificial atom coupled to two optical or microwave cavities. The two-photon process proposed in this work may have other potential applications in quantum information processing and quantum computing.

ACKNOWLEDGMENTS

This work was supported by the National Natural Science Foundation of China (NSFC; Grants No. 12004253, No. 11965017, No. 11804228, and No. U21A20436), the Jiangxi Natural Science Foundation (Grants No. 20212BAB211019, No. 20212BAB201025, and No. 20212BAB211018), the Key-Area Research and Development Program of Guangdong Province (Grant No. 2018B030326001).

APPENDIX A: DERIVATION OF THE SECOND-ORDER EFFECTIVE HAMILTONIAN $H_{\text{eff}}^{(2)}$

In this Appendix, we derive the second-order effective Hamiltonian (5) in the main text by employing James's effective Hamiltonian method [44,45]. According to Refs. [44,45], the second-order effective Hamiltonian is given by

$$H_{\text{eff}}^{(2)} = \frac{1}{i} H_I(t) \int^t H_I(t')dt'. \tag{A1}$$

In the main text, the system's interaction Hamiltonian H_I is Eq. (1), i.e.,

$$H_I = g_1(\hat{a}_1\sigma^+ e^{i\delta_1 t} + \hat{a}_1^\dagger\sigma^- e^{-i\delta_1 t}) + g_2(\hat{a}_2\sigma^+ e^{i\delta_2 t} + \hat{a}_2^\dagger\sigma^- e^{-i\delta_2 t}) + \Omega(\sigma^+ e^{i\delta_p t} + \sigma^- e^{-i\delta_p t}). \tag{A2}$$

Substituting Hamiltonian (A2) into formula (A1), we obtain

$$\begin{aligned}
H_{\text{eff}}^{(2)} &= \frac{1}{i} H_I(t) \int^t H_I(t')dt' \\
&= \frac{1}{i}[g_1(\hat{a}_1\sigma^+ e^{i\delta_1 t} + \hat{a}_1^\dagger\sigma^- e^{-i\delta_1 t}) + g_2(\hat{a}_2\sigma^+ e^{i\delta_2 t} + \hat{a}_2^\dagger\sigma^- e^{-i\delta_2 t}) + \Omega(\sigma^+ e^{i\delta_p t} + \sigma^- e^{-i\delta_p t})] \\
&\quad \times \left[\frac{g_1}{i\delta_1}(\hat{a}_1\sigma^+ e^{i\delta_1 t} - \hat{a}_1\sigma^+) - \frac{g_1}{i\delta_1}(\hat{a}_1^\dagger\sigma^- e^{-i\delta_1 t} - \hat{a}_1^\dagger\sigma^-) + \frac{g_2}{i\delta_2}(\hat{a}_2\sigma^+ e^{i\delta_2 t} - \hat{a}_2\sigma^+)\right. \\
&\quad \left. - \frac{g_2}{i\delta_2}(\hat{a}_2^\dagger\sigma^- e^{-i\delta_2 t} - \hat{a}_2^\dagger\sigma^-) + \frac{\Omega}{i\delta_p}(\sigma^+ e^{i\delta_p t} - \sigma^+) - \frac{\Omega}{i\delta_p}(\sigma^- e^{-i\delta_p t} - \sigma^-)\right] \\
&= \frac{g_1^2}{\delta_1}[\hat{a}_1\hat{a}_1^\dagger|e\rangle\langle e|(1 - e^{i\delta_1 t})] + \frac{g_1 g_2}{\delta_2}[\hat{a}_1\hat{a}_2^\dagger|e\rangle\langle e|(e^{i(\delta_1-\delta_2)t} - e^{i\delta_1 t})] \\
&\quad + \frac{g_1\Omega}{\delta_p}[\hat{a}_1|e\rangle\langle e|(e^{i(\delta_1-\delta_p)t} - e^{i\delta_1 t})] - \frac{g_1^2}{\delta_1}[\hat{a}_1^\dagger\hat{a}_1|g\rangle\langle g|(1 - e^{-i\delta_1 t})] \\
&\quad - \frac{g_1 g_2}{\delta_2}[\hat{a}_1^\dagger\hat{a}_2|g\rangle\langle g|(e^{i(\delta_2-\delta_1)t} - e^{-i\delta_1 t})] - \frac{g_1\Omega}{\delta_p}[\hat{a}_1^\dagger|g\rangle\langle g|(e^{i(\delta_p-\delta_1)t} - e^{-i\delta_1 t})] \\
&\quad + \frac{g_2^2}{\delta_2}[\hat{a}_2\hat{a}_2^\dagger|e\rangle\langle e|(1 - e^{i\delta_2 t})] + \frac{g_1 g_2}{\delta_1}[\hat{a}_1^\dagger\hat{a}_2|e\rangle\langle e|(e^{i(\delta_2-\delta_1)t} - e^{i\delta_2 t})] \\
&\quad + \frac{g_2\Omega}{\delta_p}[\hat{a}_2|e\rangle\langle e|(e^{i(\delta_2-\delta_p)t} - e^{i\delta_2 t})] - \frac{g_1 g_2}{\delta_1}[\hat{a}_1\hat{a}_2^\dagger|g\rangle\langle g|(e^{i(\delta_1-\delta_2)t} - e^{-i\delta_2 t})] \\
&\quad - \frac{g_2^2}{\delta_2}[\hat{a}_2^\dagger\hat{a}_2|g\rangle\langle g|(1 - e^{-i\delta_2 t})] - \frac{g_2\Omega}{\delta_p}[\hat{a}_2^\dagger|g\rangle\langle g|(e^{i(\delta_p-\delta_2)t} - e^{-i\delta_2 t})] \\
&\quad + \frac{g_1\Omega}{\delta_1}[\hat{a}_1^\dagger|e\rangle\langle e|(e^{i(\delta_p-\delta_1)t} - e^{i\delta_p t})] + \frac{g_2\Omega}{\delta_2}[\hat{a}_2^\dagger|e\rangle\langle e|(e^{i(\delta_p-\delta_2)t} - e^{i\delta_p t})] \\
&\quad + \frac{\Omega^2}{\delta_p}[|e\rangle\langle e|(1 - e^{i\delta_p t})] - \frac{g_1\Omega}{\delta_1}[\hat{a}_1|g\rangle\langle g|(e^{i(\delta_1-\delta_p)t} - e^{-i\delta_p t})] \\
&\quad - \frac{g_2\Omega}{\delta_2}[\hat{a}_2|g\rangle\langle g|(e^{i(\delta_2-\delta_p)t} - e^{-i\delta_p t})] - \frac{\Omega^2}{\delta_p}[|g\rangle\langle g|(1 - e^{-i\delta_p t})].
\end{aligned} \tag{A3}$$

If the dynamics are time averaged over a period much longer than the period of any of the oscillations present in the effective Hamiltonian (i.e., averaged over a time $T_a \gg 2\pi/\min\{|\delta_m - \delta_n|\}$, with $m \neq n = 1,\ 2,\ p$), the fast oscillating terms (i.e., the time-dependent terms) can be neglected by the RWA [44].

Ignoring fast oscillating terms (i.e., the time-dependent terms) using the RWA [44], we can obtain the reduced second-order effective Hamiltonian

$$\begin{aligned}
H_{\text{eff}}^{(2)} &= \frac{g_1^2}{\delta_1}(\hat{a}_1\hat{a}_1^\dagger|e\rangle\langle e| - \hat{a}_1^\dagger\hat{a}_1|g\rangle\langle g|) + \frac{g_2^2}{\delta_2}(\hat{a}_2\hat{a}_2^\dagger|e\rangle\langle e| - \hat{a}_2^\dagger\hat{a}_2|g\rangle\langle g|) + \frac{\Omega^2}{\delta_p}(|e\rangle\langle e| - |g\rangle\langle g|) \\
&= \left[\lambda_1\left(\hat{a}_1^\dagger\hat{a}_1 + \frac{1}{2}\right) + \lambda_2\left(\hat{a}_2^\dagger\hat{a}_2 + \frac{1}{2}\right) + \lambda_p\right]\sigma_z,
\end{aligned} \tag{A4}$$

which is the Hamiltonian (5) in the main text. Here, $\lambda_1 = \frac{g_1^2}{\delta_1}$, $\lambda_2 = \frac{g_2^2}{\delta_2}$, $\lambda_p = \frac{\Omega^2}{\delta_p}$, and $\sigma_z = |e\rangle\langle e| - |g\rangle\langle g|$.

APPENDIX B: DERIVATION OF THE THIRD-ORDER EFFECTIVE HAMILTONIAN $H_{\rm eff}^{(3)}$

In this Appendix, we derive the third-order effective Hamiltonians (6) in the main text by using James's effective Hamiltonian method [44,45]. In the interaction picture, the interaction Hamiltonian of the system has the form

$$H_I(t) = \sum_m \hat{h}_m \exp(i\omega_m t) + \hat{h}_m^\dagger \exp(-i\omega_m t). \tag{B1}$$

Consider the third-order case and assume that all of the frequencies ω_m are distinct and the algebraic sum of any three frequencies is equal to zero or distinct from zero. By using the RWA, one can obtain a third-order James's effective Hamiltonian [45],

$$\begin{aligned} H_{\rm eff}^{(3)}(t) = \sum_{l,m,n} \Bigg\{ & \frac{1}{\omega_n(\omega_n-\omega_m)}[\hat{h}_l\hat{h}_m^\dagger\hat{h}_n e^{i(\omega_l-\omega_m+\omega_n)t} + \hat{h}_l^\dagger\hat{h}_m\hat{h}_n^\dagger e^{i(-\omega_l+\omega_m-\omega_n)t} + \hat{h}_l\hat{h}_m\hat{h}_n^\dagger e^{i(\omega_l+\omega_m-\omega_n)t} + \hat{h}_l^\dagger\hat{h}_m^\dagger\hat{h}_n e^{i(-\omega_l-\omega_m+\omega_n)t}] \\ & + \frac{1}{\omega_n(\omega_n+\omega_m)}[\hat{h}_l^\dagger\hat{h}_m\hat{h}_n e^{i(-\omega_l+\omega_m+\omega_n)t} + \hat{h}_l\hat{h}_m^\dagger\hat{h}_n^\dagger e^{i(\omega_l-\omega_m-\omega_n)t}] \Bigg\}. \end{aligned} \tag{B2}$$

In our main text, the interaction Hamiltonian of the system is given by Eq. (1), i.e.,

$$H_I = g_1(\hat{a}_1\sigma^+ e^{i\delta_1 t} + \hat{a}_1^\dagger\sigma^- e^{-i\delta_1 t}) + g_2(\hat{a}_2\sigma^+ e^{i\delta_2 t} + \hat{a}_2^\dagger\sigma^- e^{-i\delta_2 t}) + \Omega(\sigma^+ e^{i\delta_p t} + \sigma^- e^{-i\delta_p t}). \tag{B3}$$

According to Eqs. (B1) and (B2), we choose $\hat{h}_1 = g_1\hat{a}_1\sigma^+$, $\omega_1 = \delta_1$; $\hat{h}_2 = g_2\hat{a}_2\sigma^+$, $\omega_2 = \delta_2$; and $\hat{h}_3 = \Omega\sigma^+$, $\omega_3 = \delta_p$. Thus, in the dispersive regimes $\delta_1 \gg g_1$, $\delta_2 \gg g_2$, and $\delta_p \gg \Omega$, we can obtain the third-order James's effective Hamiltonian according to formula (B2) [45]:

$$\begin{aligned} H_{\rm eff}^{(3)} = & \frac{1}{\omega_3(\omega_3-\omega_2)}[\hat{h}_1\hat{h}_2^\dagger\hat{h}_3 e^{i(\omega_1-\omega_2+\omega_3)t} + \hat{h}_1^\dagger\hat{h}_2\hat{h}_3^\dagger e^{-i(\omega_1-\omega_2+\omega_3)t} + \hat{h}_1\hat{h}_2\hat{h}_3^\dagger e^{i(\omega_1+\omega_2-\omega_3)t} + \hat{h}_1^\dagger\hat{h}_2^\dagger\hat{h}_3 e^{-i(\omega_1+\omega_2-\omega_3)t}] \\ & + \frac{1}{\omega_3(\omega_3+\omega_2)}[\hat{h}_1^\dagger\hat{h}_2\hat{h}_3 e^{i(-\omega_1+\omega_2+\omega_3)t} + \hat{h}_1\hat{h}_2^\dagger\hat{h}_3^\dagger e^{-i(-\omega_1+\omega_2+\omega_3)t}] \\ & + \frac{1}{\omega_2(\omega_2-\omega_3)}[\hat{h}_1\hat{h}_3^\dagger\hat{h}_2 e^{i(\omega_1-\omega_3+\omega_2)t} + \hat{h}_1^\dagger\hat{h}_3\hat{h}_2^\dagger e^{-i(\omega_1-\omega_3+\omega_2)t} + \hat{h}_1\hat{h}_3\hat{h}_2^\dagger e^{i(\omega_1+\omega_3-\omega_2)t} + \hat{h}_1^\dagger\hat{h}_3^\dagger\hat{h}_2 e^{-i(\omega_1+\omega_3-\omega_2)t}] \\ & + \frac{1}{\omega_2(\omega_2+\omega_3)}[\hat{h}_1^\dagger\hat{h}_3\hat{h}_2 e^{i(-\omega_1+\omega_3+\omega_2)t} + \hat{h}_1\hat{h}_3^\dagger\hat{h}_2^\dagger e^{-i(-\omega_1+\omega_3+\omega_2)t}] \\ & + \frac{1}{\omega_3(\omega_3-\omega_1)}[\hat{h}_2\hat{h}_1^\dagger\hat{h}_3 e^{i(\omega_2-\omega_1+\omega_3)t} + \hat{h}_2^\dagger\hat{h}_1\hat{h}_3^\dagger e^{-i(\omega_2-\omega_1+\omega_3)t} + \hat{h}_2\hat{h}_1\hat{h}_3^\dagger e^{i(\omega_2+\omega_1-\omega_3)t} + \hat{h}_2^\dagger\hat{h}_1^\dagger\hat{h}_3 e^{-i(\omega_2+\omega_1-\omega_3)t}] \\ & + \frac{1}{\omega_3(\omega_3+\omega_1)}[\hat{h}_2^\dagger\hat{h}_1\hat{h}_3 e^{i(-\omega_2+\omega_1+\omega_3)t} + \hat{h}_2\hat{h}_1^\dagger\hat{h}_3^\dagger e^{-i(-\omega_2+\omega_1+\omega_3)t}] \\ & + \frac{1}{\omega_1(\omega_1-\omega_3)}[\hat{h}_2\hat{h}_3^\dagger\hat{h}_1 e^{i(\omega_2-\omega_3+\omega_1)t} + \hat{h}_2^\dagger\hat{h}_3\hat{h}_1^\dagger e^{-i(\omega_2-\omega_3+\omega_1)t} + \hat{h}_2\hat{h}_3\hat{h}_1^\dagger e^{i(\omega_2+\omega_3-\omega_1)t} + \hat{h}_2^\dagger\hat{h}_3^\dagger\hat{h}_1 e^{-i(\omega_2+\omega_3-\omega_1)t}] \\ & + \frac{1}{\omega_1(\omega_1+\omega_3)}[\hat{h}_2^\dagger\hat{h}_3\hat{h}_1 e^{i(-\omega_2+\omega_3+\omega_1)t} + \hat{h}_2\hat{h}_3^\dagger\hat{h}_1^\dagger e^{-i(-\omega_2+\omega_3+\omega_1)t}] \\ & + \frac{1}{\omega_2(\omega_2-\omega_1)}[\hat{h}_3\hat{h}_1^\dagger\hat{h}_2 e^{i(\omega_3-\omega_1+\omega_2)t} + \hat{h}_3^\dagger\hat{h}_1\hat{h}_2^\dagger e^{-i(\omega_3-\omega_1+\omega_2)t} + \hat{h}_3\hat{h}_1\hat{h}_2^\dagger e^{i(\omega_3+\omega_1-\omega_2)t} + \hat{h}_3^\dagger\hat{h}_1^\dagger\hat{h}_2 e^{-i(\omega_3+\omega_1-\omega_2)t}] \\ & + \frac{1}{\omega_2(\omega_2+\omega_1)}[\hat{h}_3^\dagger\hat{h}_1\hat{h}_2 e^{i(-\omega_3+\omega_1+\omega_2)t} + \hat{h}_3\hat{h}_1^\dagger\hat{h}_2^\dagger e^{-i(-\omega_3+\omega_1+\omega_2)t}] \\ & + \frac{1}{\omega_1(\omega_1-\omega_2)}[\hat{h}_3\hat{h}_2^\dagger\hat{h}_1 e^{i(\omega_3-\omega_2+\omega_1)t} + \hat{h}_3^\dagger\hat{h}_2\hat{h}_1^\dagger e^{-i(\omega_3-\omega_2+\omega_1)t} + \hat{h}_3\hat{h}_2\hat{h}_1^\dagger e^{i(\omega_3+\omega_2-\omega_1)t} + \hat{h}_3^\dagger\hat{h}_2^\dagger\hat{h}_1 e^{-i(\omega_3+\omega_2-\omega_1)t}] \\ & + \frac{1}{\omega_1(\omega_1+\omega_2)}[\hat{h}_3^\dagger\hat{h}_2\hat{h}_1 e^{i(-\omega_3+\omega_2+\omega_1)t} + \hat{h}_3\hat{h}_2^\dagger\hat{h}_1^\dagger e^{-i(-\omega_3+\omega_2+\omega_1)t}]. \end{aligned} \tag{B4}$$

Assuming that $\omega_3 \gg \omega_1 > \omega_2$ (i.e., $\delta_p \gg \delta_1 > \delta_2$) and satisfying $\omega_3 \gtrsim \omega_1 + \omega_2$ (i.e., $\delta_p \gtrsim \delta_1 + \delta_2$), we can drop the fast oscillating terms using the RWA. Keeping only the slowly oscillating terms with the factors $e^{i(\omega_3-\omega_1-\omega_2)t}$ and $e^{-i(\omega_3-\omega_1-\omega_2)t}$, the effective Hamiltonian $H_{\rm eff}^{(3)}$ can be approximated as

$$\begin{aligned} H_{\rm eff}^{(3)} = & \frac{1}{\omega_3(\omega_3-\omega_2)}[\hat{h}_1\hat{h}_2\hat{h}_3^\dagger e^{i(\omega_1+\omega_2-\omega_3)t} + \hat{h}_1^\dagger\hat{h}_2^\dagger\hat{h}_3 e^{-i(\omega_1+\omega_2-\omega_3)t}] + \frac{1}{\omega_2(\omega_2-\omega_3)}[\hat{h}_1\hat{h}_3^\dagger\hat{h}_2 e^{i(\omega_1-\omega_3+\omega_2)t} + \hat{h}_1^\dagger\hat{h}_3\hat{h}_2^\dagger e^{-i(\omega_1-\omega_3+\omega_2)t}] \\ & + \frac{1}{\omega_3(\omega_3-\omega_1)}[\hat{h}_2\hat{h}_1\hat{h}_3^\dagger e^{i(\omega_2+\omega_1-\omega_3)t} + \hat{h}_2^\dagger\hat{h}_1^\dagger\hat{h}_3 e^{-i(\omega_2+\omega_1-\omega_3)t}] + \frac{1}{\omega_1(\omega_1-\omega_3)}[\hat{h}_2\hat{h}_3^\dagger\hat{h}_1 e^{i(\omega_2-\omega_3+\omega_1)t} + \hat{h}_2^\dagger\hat{h}_3\hat{h}_1^\dagger e^{-i(\omega_2-\omega_3+\omega_1)t}] \end{aligned}$$

$$+\frac{1}{\omega_2(\omega_2+\omega_1)}[\hat{h}_3^\dagger\hat{h}_1\hat{h}_2e^{i(-\omega_3+\omega_1+\omega_2)t}+\hat{h}_3\hat{h}_1^\dagger\hat{h}_2^\dagger e^{-i(-\omega_3+\omega_1+\omega_2)t}]$$
$$+\frac{1}{\omega_1(\omega_1+\omega_2)}[\hat{h}_3^\dagger\hat{h}_2\hat{h}_1e^{i(-\omega_3+\omega_2+\omega_1)t}+\hat{h}_3\hat{h}_2^\dagger\hat{h}_1^\dagger e^{-i(-\omega_3+\omega_2+\omega_1)t}]$$
$$=\frac{g_1g_2\Omega}{\delta_2(\delta_2-\delta_p)}[\hat{a}_1\hat{a}_2\sigma^+e^{i(\delta_1-\delta_p+\delta_2)t}+\hat{a}_1^\dagger\hat{a}_2^\dagger\sigma^-e^{-i(\delta_1-\delta_p+\delta_2)t}]+\frac{g_1g_2\Omega}{\delta_1(\delta_1-\delta_p)}[\hat{a}_1\hat{a}_2\sigma^+e^{i(\delta_2-\delta_p+\delta_1)t}+\hat{a}_1^\dagger\hat{a}_2^\dagger\sigma^-e^{-i(\delta_2-\delta_p+\delta_1)t}], \tag{B5}$$

where we have used $\sigma^-\sigma^-=0$ and $\sigma^+\sigma^+=0$. Accordingly, the Hamiltonian (B5) can be reduced to

$$H_{\rm eff}^{(3)}=-g(\hat{a}_1\hat{a}_2\sigma^+e^{-i\Delta t}+\hat{a}_1^\dagger\hat{a}_2^\dagger\sigma^-e^{i\Delta t}), \tag{B6}$$

which is the Hamiltonian (6) in the main text. Here, $\Delta=\delta_p-\delta_1-\delta_2$, $g=g_1g_2\Omega[\frac{1}{\delta_2(\delta_p-\delta_2)}+\frac{1}{\delta_1(\delta_p-\delta_1)}]$.

From Eq. (B4), we can obtain the fourth-order effective Hamiltonian,

$$\begin{aligned}
H_{\rm eff}^{(4)}&=-\frac{1}{i}H_I(t)\int^t H_I(t_1)\int^{t_1}H_I(t_2)\int^{t_2}H_I(t_3)dt_3dt_2dt_1\\
&=\frac{g_1\chi_1}{\delta_1-\delta_2+\delta_p}[-\hat{a}_1\hat{a}_1^\dagger\hat{a}_2|e\rangle\langle e|e^{-i(\delta_p-\delta_2)t}+\hat{a}_1\hat{a}_1^\dagger\hat{a}_2|e\rangle\langle e|e^{i\delta_1t}+\hat{a}_1^\dagger\hat{a}_1\hat{a}_2^\dagger|g\rangle\langle g|e^{i(\delta_p-\delta_2)t}-\hat{a}_1^\dagger\hat{a}_1\hat{a}_2^\dagger|g\rangle\langle g|e^{-i\delta_1t}]\\
&+\frac{g_1\chi_2}{\delta_p-\delta_1+\delta_2}[-\hat{a}_1\hat{a}_1\hat{a}_2^\dagger|e\rangle\langle e|e^{-i(\delta_p-2\delta_1+\delta_2)t}+\hat{a}_1\hat{a}_1\hat{a}_2^\dagger|e\rangle\langle e|e^{i\delta_1t}+\hat{a}_1^\dagger\hat{a}_1^\dagger\hat{a}_2|g\rangle\langle g|e^{i(\delta_p-2\delta_1+\delta_2)t}-\hat{a}_1^\dagger\hat{a}_1^\dagger\hat{a}_2|g\rangle\langle g|e^{-i\delta_1t}]\\
&+\frac{g_1g}{\delta_p-\delta_1-\delta_2}[-\hat{a}_1\hat{a}_1^\dagger\hat{a}_2^\dagger|e\rangle\langle e|e^{-i(-\delta_p+\delta_2)t}+\hat{a}_1\hat{a}_1^\dagger\hat{a}_2^\dagger|e\rangle\langle e|e^{i\delta_1t}+\hat{a}_1^\dagger\hat{a}_1\hat{a}_2|g\rangle\langle g|e^{i(-\delta_p+\delta_2)t}-\hat{a}_1^\dagger\hat{a}_1\hat{a}_2|g\rangle\langle g|e^{-i\delta_1t}]\\
&+\frac{g_2\chi_1}{\delta_1-\delta_2+\delta_p}[-\hat{a}_1^\dagger\hat{a}_2\hat{a}_2|e\rangle\langle e|e^{-i(\delta_1-2\delta_2+\delta_p)t}+\hat{a}_1^\dagger\hat{a}_2\hat{a}_2|e\rangle\langle e|e^{i\delta_2t}+\hat{a}_1\hat{a}_2^\dagger\hat{a}_2^\dagger|g\rangle\langle g|e^{i(\delta_1-2\delta_2+\delta_p)t}-\hat{a}_1\hat{a}_2^\dagger\hat{a}_2^\dagger|g\rangle\langle g|e^{-i\delta_2t}]\\
&+\frac{g_2\chi_2}{\delta_p-\delta_1+\delta_2}[-\hat{a}_1\hat{a}_2\hat{a}_2^\dagger|e\rangle\langle e|e^{-i(\delta_p-\delta_1)t}+\hat{a}_1\hat{a}_2\hat{a}_2^\dagger|e\rangle\langle e|e^{i\delta_2t}+\hat{a}_1^\dagger\hat{a}_2^\dagger\hat{a}_2|g\rangle\langle g|e^{i(\delta_p-\delta_1)t}-\hat{a}_1^\dagger\hat{a}_2^\dagger\hat{a}_2|g\rangle\langle g|e^{-i\delta_2t}]\\
&+\frac{g_2g}{\delta_p-\delta_1-\delta_2}[-\hat{a}_1^\dagger\hat{a}_2\hat{a}_2^\dagger|e\rangle\langle e|e^{-i(\delta_1-\delta_p)t}+\hat{a}_1^\dagger\hat{a}_2\hat{a}_2^\dagger|e\rangle\langle e|e^{i\delta_2t}+\hat{a}_1\hat{a}_2^\dagger\hat{a}_2|g\rangle\langle g|e^{i(\delta_1-\delta_p)t}-\hat{a}_1\hat{a}_2^\dagger\hat{a}_2|g\rangle\langle g|e^{-i\delta_2t}]\\
&+\frac{\Omega\chi_1}{\delta_1-\delta_2+\delta_p}[-\hat{a}_1^\dagger\hat{a}_2|e\rangle\langle e|e^{-i(\delta_1-\delta_2)t}+\hat{a}_1^\dagger\hat{a}_2|e\rangle\langle e|e^{i\delta_pt}+\hat{a}_1\hat{a}_2^\dagger|g\rangle\langle g|e^{i(\delta_1-\delta_2)t}-\hat{a}_1\hat{a}_2^\dagger|g\rangle\langle g|e^{-i\delta_pt}]\\
&+\frac{\Omega\chi_2}{\delta_p-\delta_1+\delta_2}[-\hat{a}_1\hat{a}_2^\dagger|e\rangle\langle e|e^{-i(-\delta_1+\delta_2)t}+\hat{a}_1\hat{a}_2^\dagger|e\rangle\langle e|e^{i\delta_pt}+\hat{a}_1^\dagger\hat{a}_2|g\rangle\langle g|e^{i(-\delta_1+\delta_2)t}-\hat{a}_1^\dagger\hat{a}_2|g\rangle\langle g|e^{-i\delta_pt}]\\
&+\frac{\Omega g}{\delta_p-\delta_1-\delta_2}[-\hat{a}_1^\dagger\hat{a}_2^\dagger|e\rangle\langle e|e^{-i(\delta_1-2\delta_p+\delta_2)t}+\hat{a}_1^\dagger\hat{a}_2^\dagger|e\rangle\langle e|e^{i\delta_pt}+\hat{a}_1\hat{a}_2|g\rangle\langle g|e^{i(\delta_1-2\delta_p+\delta_2)t}-\hat{a}_1\hat{a}_2|g\rangle\langle g|e^{-i\delta_pt}],
\end{aligned} \tag{B7}$$

where $\chi_1=g_1g_2\Omega[\frac{1}{\delta_p(\delta_p-\delta_2)}+\frac{1}{\delta_1(\delta_1-\delta_2)}]$ and $\chi_2=g_1g_2\Omega[\frac{1}{\delta_p(\delta_p-\delta_1)}-\frac{1}{\delta_2(\delta_1-\delta_2)}]$. Typically, under the condition $\delta_p\gg\delta_1>\delta_2$ and satisfying $\delta_p+\delta_2\ll2\delta_1$, the fourth-order terms can be neglected using the RWA. According to the condition $\delta_p\gtrsim\delta_1+\delta_2$ given above, we can obtain $\delta_1\gg2\delta_2$ (i.e., $\delta_p\gg3\delta_2$). Alternatively, when the third-order effective coupling strength is far greater than the fourth-order effective coupling constants, i.e., $g\gg\{\frac{g_1\chi_1}{\delta_1-\delta_2+\delta_p},\ \frac{g_1\chi_2}{\delta_p-\delta_1+\delta_2},\ \ldots,\ \frac{\Omega g}{\delta_p-\delta_1-\delta_2}\}$, the fourth-order terms can also be neglected. However, these conditions do not need to be met when the Hilbert space is expanded in the basis states $|e\rangle|0\rangle_1|0\rangle_2$ and $|g\rangle|1\rangle_1|1\rangle_2$. In the states $|e\rangle|0\rangle_1|0\rangle_2$ and $|g\rangle|1\rangle_1|1\rangle_2$, we can easily obtain $\langle e|\langle0|\langle0|H_{\rm eff}^{(4)}|e\rangle|0\rangle|0\rangle=0$, $\langle e|\langle0|\langle0|H_{\rm eff}^{(4)}|g\rangle|1\rangle|1\rangle=0$, $\langle g|\langle1|\langle1|H_{\rm eff}^{(4)}|e\rangle|0\rangle|0\rangle=0$, and $\langle g|\langle1|\langle1|H_{\rm eff}^{(4)}|g\rangle|1\rangle|1\rangle=0$. Thus, when the Hilbert space is expanded in the states $|e\rangle|0\rangle_1|0\rangle_2$ and $|g\rangle|1\rangle_1|1\rangle_2$, the fourth-order terms can be neglected.

[1] M. Göppert-Mayer, Über elementarakte mit zwei quantensprüngen, Ann. Phys. (Berlin, Ger.) **401**, 273 (1931).

[2] W. Denk, J. Strickler, and W. Webb, Two-photon laser scanning fluorescence microscopy, Science **248**, 73 (1990).

[3] Y. M. He, H. Wang, C. Wang, M. C. Chen, X. Ding, J. Qin, Z. C. Duan, S. Chen, J. P. Li, R. Z. Liu, C. Schneider, M. Atatüre, S. Höfling, C. Y. Lu, and J. W. Pan, Coherently driving a single quantum two-level system with dichromatic laser pulses, Nat. Phys. **15**, 941 (2019).

[4] S. Maruo, O. Nakamura, and S. Kawata, Three-dimensional microfabrication with two-photon-absorbed photopolymerization, Opt. Lett. **22**, 132 (1997).

[5] M. Brune, J. M. Raimond, P. Goy, L. Davidovich, and S. Haroche, Realization of a Two-Photon Maser Oscillator, Phys. Rev. Lett. **59**, 1899 (1987).

[6] S. C. Gou, Quantum behavior of a two-level atom interacting with two modes of light in a cavity, Phys. Rev. A **40**, 5116 (1989).

[7] M. M. Ashraf, Cavity field spectra of the nondegenerate two-photon Jaynes-Cummings model, Phys. Rev. A **50**, 5116 (1994).

[8] P. A. M. Neto, L. Davidovich, and J. M. Raimond, Theory of the nondegenerate two-photon micromaser, Phys. Rev. A **43**, 5073 (1991).

[9] Y. Wu and X. Yang, Effective two-level model for a three-level atom in the Ξ configuration, Phys. Rev. A **56**, 2443 (1997).

[10] L. Garziano, V. Macrì, R. Stassi, O. D. Stefano, F. Nori, and S. Savasta, One Photon Can Simultaneously Excite Two or More Atoms, Phys. Rev. Lett. **117**, 043601 (2016).

[11] P. Zhao, X. Tan, H. Yu, S. L. Zhu, and Y. Yu, Simultaneously exciting two atoms with photon-mediated Raman interactions, Phys. Rev. A **95**, 063848 (2017).

[12] X. Wang, A. Miranowicz, H. R. Li, and F. Nori, Observing pure effects of counter-rotating terms without ultrastrong coupling: A single photon can simultaneously excite two qubits, Phys. Rev. A **96**, 063820 (2017).

[13] R. Stassi, V. Macrì, A. F. Kockum, O. D. Stefano, A. Miranowicz, S. Savasta, and F. Nori, Quantum nonlinear optics without photons, Phys. Rev. A **96**, 023818 (2017).

[14] P. Zhao, X. Tan, H. Yu, S. L. Zhu, and Y. Yu, Circuit QED with qutrits: Coupling three or more atoms via virtual-photon exchange, Phys. Rev. A **96**, 043833 (2017).

[15] W. Ren, W. Liu, C. Song, H. Li, Q. Guo, Z. Wang, D. Zheng, G. S. Agarwal, M. O. Scully, S. Y. Zhu, H. Wang, and D. W. Wang, Simultaneous Excitation of Two Noninteracting Atoms with Time-Frequency Correlated Photon Pairs in a Superconducting Circuit, Phys. Rev. Lett. **125**, 133601 (2020).

[16] D. P. DiVincenzo and P. W. Shor, Fault-Tolerant Error Correction with Efficient Quantum Codes, Phys. Rev. Lett. **77**, 3260 (1996).

[17] A. Karlsson and M. Bourennane, Quantum teleportation using three-particle entanglement, Phys. Rev. A **58**, 4394 (1998).

[18] V. Giovannetti, S. Lloyd, and L. Maccon, Quantum-enhanced measurements: Beating the standard quantum limit, Science **306**, 1330 (2004).

[19] J. Brendel, N. Gisin, W. Tittel, and H. Zbinden, Pulsed Energy-Time Entangled Twin-Photon Source for Quantum Communication, Phys. Rev. Lett. **82**, 2594 (1999).

[20] J. W. Pan, D. Bouwmeester, H. Weinfurter, and A. Zeilinger, Experimental Entanglement Swapping: Entangling Photons That Never Interacted, Phys. Rev. Lett. **80**, 3891 (1998).

[21] N. D. Mermin, Extreme Quantum Entanglement in a Superposition of Macroscopically Distinct States, Phys. Rev. Lett. **65**, 1838 (1990).

[22] C. P. Yang and S. Han, Preparation of Greenberger-Horne-Zeilinger entangled states with multiple superconducting quantum-interference device qubits or atoms in cavity QED, Phys. Rev. A **70**, 062323 (2004).

[23] S. L. Zhu, Z. D. Wang, and P. Zanardi, Geometric Quantum Computation and Multiqubit Entanglement with Superconducting Qubits Inside a Cavity, Phys. Rev. Lett. **94**, 100502 (2005).

[24] Y. D. Wang, S. Chesi, D. Loss, and C. Bruder, One-step multiqubit Greenberger-Horne-Zeilinger state generation in a circuit QED system, Phys. Rev. B **81**, 104524 (2010).

[25] W. Feng, P. Wang, X. Ding, L. Xu, and X. Q. Li, Generating and stabilizing the Greenberger-Horne-Zeilinger state in circuit QED: Joint measurement, Zeno effect, and feedback, Phys. Rev. A **83**, 042313 (2011).

[26] S. Aldana, Y. D. Wang, and C. Bruder, Greenberger-Horne-Zeilinger generation protocol for N superconducting transmon qubits capacitively coupled to a quantum bus, Phys. Rev. B **84**, 134519 (2011).

[27] C. P. Yang, Q. P. Su, and S. Han, Generation of Greenberger-Horne-Zeilinger entangled states of photons in multiple cavities via a superconducting qutrit or an atom through resonant interaction, Phys. Rev. A **86**, 022329 (2012).

[28] C. P. Yang, Q. P. Su, S. B. Zheng, and S. Han, Generating entanglement between microwave photons and qubits in multiple cavities coupled by a superconducting qutrit, Phys. Rev. A **87**, 022320 (2013).

[29] X. T. Mo and Z. Y. Xue, Single-step multipartite entangled states generation from coupled circuit cavities, Front. Phys. **14**, 31602 (2019).

[30] T. Liu, Q. P. Su, Y. Zhang, Y. L. Fang, and C. P. Yang, Generation of quantum entangled states of multiple groups of qubits distributed in multiple cavities, Phys. Rev. A **101**, 012337 (2020).

[31] Y. Zhang, T. Liu, J. Zhao, Y. Yu, and C. P. Yang, Generation of hybrid Greenberger-Horne-Zeilinger entangled states of particlelike and wavelike optical qubits in circuit QED, Phys. Rev. A **101**, 062334 (2020).

[32] C. S. Yu, X. X. Yi, H. S. Song, and D. Mei, Robust preparation of Greenberger-Horne-Zeilinger and W states of three distant atoms, Phys. Rev. A **75**, 044301 (2007).

[33] Q. C. Wu, Y. H. Zhou, B. L. Ye, T. Liu, J. L. Zhao, D. X. Chen, and C. P. Yang, Generation of an enhanced multi-mode optomechanical-like quantum system and its application in creating hybrid entangled states, Ann. Phys. (Berlin, Ger.) **534**, 2100393 (2022).

[34] S. F. Qi and J. Jing, Generation of Bell and Greenberger-Horne-Zeilinger states from a hybrid qubit-photon-magnon system, Phys. Rev. A **105**, 022624 (2022).

[35] P. Neumann, N. Mizuochi, F. Rempp, P. Hemmer, H. Watanabe, S. Yamasaki, V. Jacques, T. Gaebel, F. Jelezko, and J. Wrachtrup, Multipartite entanglement among single spins in diamond, Science **320**, 1326 (2008).

[36] H. S. Zhong, Y. Li, W. Li, L. C. Peng, Z. E. Su, Y. Hu, Y. M. He, X. Ding, W. Zhang, H. Li, L. Zhang, Z. Wang, L. You, X. L. Wang, X. Jiang, L. Li, Y. A. Chen, N. L. Liu, C. Y. Lu, and J. W. Pan, 12-Photon Entanglement and Scalable Scattershot Boson Sampling with Optimal Entangled-Photon Pairs from Parametric Down-Conversion, Phys. Rev. Lett. **121**, 250505 (2018).

[37] X.-L. Wang, Y.-H. Luo, H.-L. Huang, M.-C. Chen, Z.-E. Su, C. Liu, C. Chen, W. Li, Y.-Q. Fang, X. Jiang, J. Zhang, L. Li, N.-L. Liu, C.-Y. Lu, and J.-W. Pan, 18-Qubit Entanglement with Six Photons' Three Degrees of Freedom, Phys. Rev. Lett. **120**, 260502 (2018).

[38] T. Monz, P. Schindler, J. T. Barreiro, M. Chwalla, D. Nigg, W. A. Coish, M. Harlander, W. Hansel, M. Hennrich, and R. Blatt, 14-Qubit Entanglement: Creation and Coherence, Phys. Rev. Lett. **106**, 130506 (2011).

[39] A. Omran, H. Levine, A. Keesling, G. Semeghini, T. T. Wang, S. Ebadi, H. Bernien, A. S. Zibrov, H. Pichler, S. Choi, J. Cui,

M. Rossignolo, P. Rembold, S. Montangero, T. Calarco, M. Endres, M. Greiner, V. Vuletić, and M. D. Lukin, Generation and manipulation of Schrödinger cat states in Rydberg atom arrays, Science **365**, 570 (2019).

[40] M. Neeley, R. C. Bialczak, M. Lenander, E. Lucero, M. Mariantoni, A. D. O'Connell, D. Sank, H. Wang, M. Weides, J. Wenner, Y. Yin, T. Yamamoto, A. N. Cleland, and J. M. Martinis, Generation of three-qubit entangled states using superconducting phase qubits, Nature (London) **467**, 570 (2010).

[41] C. Song, K. Xu, W. Liu, C. P. Yang, S. B. Zheng, H. Deng, Q. Xie, K. Huang, Q. Guo, L. Zhang, P. Zhang, D. Xu, D. Zheng, X. Zhu, H. Wang, Y. A. Chen, C. Y. Lu, S. Han, and J. W. Pan, 10-Qubit Entanglement and Parallel Logic Operations with a Superconducting Circuit, Phys. Rev. Lett. **119**, 180511 (2017).

[42] M. Gong *et al.*, Genuine 12-Qubit Entanglement on a Superconducting Quantum Processor, Phys. Rev. Lett. **122**, 110501 (2019).

[43] C. Song, K. Xu, H. Li, Y.-R. Zhang, X. Zhang, W. Liu, Q. Guo, Z. Wang, W. Ren, J. Hao, H. Feng, H. Fan, D. Zheng, D.-W. Wang, H. Wang, and S.-Y. Zhu, Generation of multicomponent atomic Schrödinger cat states of up to 20 qubits, Science **365**, 574 (2019).

[44] D. F. V. James, Quantum computation with hot and cold ions: An assessment of proposed schemes, Fortschr. Phys. **48**, 823 (2000).

[45] W. Shao, C. Wu, and X. L. Feng, Generalized James' effective Hamiltonian method, Phys. Rev. A **95**, 032124 (2017).

[46] A. Sørensen and K. Mølmer, Quantum Computation with Ions in Thermal Motion, Phys. Rev. Lett. **82**, 1971 (1999).

[47] S. B. Zheng and G. C. Guo, Efficient Scheme for Two-Atom Entanglement and Quantum Information Processing in Cavity QED, Phys. Rev. Lett. **85**, 2392 (2000).

[48] N. Zagury, A. Aragão, J. Casanova, and E. Solano, Unitary expansion of the time evolution operator, Phys. Rev. A **82**, 042110 (2010).

[49] F. O. Prado, N. G. de Almeida, M. H. Y. Moussa, and C. J. Villas-Bôas, Bilinear and quadratic Hamiltonians in two-mode cavity quantum electrodynamics, Phys. Rev. A **73**, 043803 (2006).

[50] F. O. Prado, F. S. Luiz, J. M. Villas-Bôas, A. M. Alcalde, E. I. Duzzioni, and L. Sanz, Atom-mediated effective interactions between modes of a bimodal cavity, Phys. Rev. A **84**, 053839 (2011).

[51] C. P. Yang, S. I. Chu, and S. Han, Possible realization of entanglement, logical gates, and quantum information transfer with superconducting-quantum-interference-device qubits in cavity QED, Phys. Rev. A **67**, 042311 (2003).

[52] J. Q. You and F. Nori, Quantum information processing with superconducting qubits in a microwave field, Phys. Rev. B **68**, 064509 (2003).

[53] A. Blais, R. S. Huang, A. Wallra, S. M. Girvin, and R. J. Schoelkopf, Cavity quantum electrodynamics for superconducting electrical circuits: An architecture for quantum computation, Phys. Rev. A **69**, 062320 (2004).

[54] J. Clarke and F. K. Wilhelm, Superconducting quantum bits, Nature (London) **453**, 1031 (2008).

[55] J. Q. You and F. Nori, Atomic physics and quantum optics using superconducting circuits, Nature (London) **474**, 589 (2011).

[56] M. H. Devoret and R. J. Schoelkopf, Superconducting circuits for quantum information: An outlook, Science **339**, 1169 (2013).

[57] X. Gu, A. F. Kockum, A. Miranowicz, Y. X. Liu, and F. Nori, Microwave photonics with superconducting quantum circuits, Phys. Rep. **718–719**, 1 (2017).

[58] A. Blais, S. M. Girvin, and W. D. Oliver, Quantum information processing and quantum optics with circuit quantum electrodynamics, Nat. Phys. **16**, 247 (2020).

[59] C. P. Yang, S. I. Chu, and S. Han, Quantum Information Transfer and Entanglement with SQUID Qubits in Cavity QED: A Dark-State Scheme with Tolerance for Nonuniform Device Parameter, Phys. Rev. Lett. **92**, 117902 (2004).

[60] Z. Kis and E. Paspalakis, Arbitrary rotation and entanglement of flux SQUID qubits, Phys. Rev. B **69**, 024510 (2004).

[61] Y. D. Wang, Z. D. Wang, and C. P. Sun, Quantum storage and information transfer with superconducting qubits, Phys. Rev. B **72**, 172507 (2005).

[62] F. W. Strauch and C. J. Williams, Theoretical analysis of perfect quantum state transfer with superconducting qubits, Phys. Rev. B **78**, 094516 (2008).

[63] C. P. Yang, Q. P. Su, and F. Nori, Entanglement generation and quantum information transfer between spatially-separated qubits in different cavities, New J. Phys. **15**, 115003 (2013).

[64] P. M. Billangeon, J. S. Tsai, and Y. Nakamura, Circuit-QED-based scalable architectures for quantum information processing with superconducting qubits, Phys. Rev. B **91**, 094517 (2015).

[65] T. Liu, Z. F. Zheng, Y. Zhang, Y. L. Fang, and C. P. Yang, Transferring entangled states of photonic cat-state qubits in circuit QED, Front. Phys. **15**, 21603 (2020).

[66] K. H. Song, Z. W. Zhou, and G. C. Guo, Quantum logic gate operation and entanglement with superconducting quantum interference devices in a cavity via a Raman transition, Phys. Rev. A **71**, 052310 (2005).

[67] T. Tanamoto, Y. Liu, S. Fujita, X. Hu, and F. Nori, Producing Cluster States in Charge Qubits and Flux Qubits, Phys. Rev. Lett. **97**, 230501 (2006).

[68] X. L. Zhang, K. L. Gao, and M. Feng, Preparation of cluster states and W states with superconducting quantum-interference-device qubits in cavity QED, Phys. Rev. A **74**, 024303 (2006).

[69] P. B. Li, S. Y. Gao, and F. L. Li, Engineering two-mode entangled states between two superconducting resonators by dissipation, Phys. Rev. A **86**, 012318 (2012).

[70] T. Liu, Q. P. Su, S. J. Xiong, J. M. Liu, C. P. Yang, and F. Nori, Generation of a macroscopic entangled coherent state using quantum memories in circuit QED, Sci. Rep. **6**, 32004 (2016).

[71] Y. H. Kang, Y. H. Chen, Z. C. Shi, J. Song, and Y. Xia, Fast preparation of W states with superconducting quantum interference devices by using dressed states, Phys. Rev. A **94**, 052311 (2016).

[72] C. P. Yang and S. Han, n-qubit-controlled phase gate with superconducting quantum-interference devices coupled to a resonator, Phys. Rev. A **72**, 032311 (2005).

[73] C. P. Yang, Y. Liu, and F. Nori, Phase gate of one qubit simultaneously controlling n qubits in a cavity, Phys. Rev. A **81**, 062323 (2010).

[74] C. P. Yang, Q. P. Su, F. Y. Zhang, and S. B. Zheng, Single-step implementation of a multiple-target-qubit controlled phase

gate without need of classical pulses, Opt. Lett. **39**, 3312 (2014).

[75] T. Liu, X. Z. Cao, Q. P. Su, S. J. Xiong, and C. P. Yang, Multi-target-qubit unconventional geometric phase gate in a multi-cavity system, Sci. Rep. **6**, 21562 (2016).

[76] T. Liu, B. Q. Guo, C. S. Yu, and W. N. Zhang, One-step implementation of a hybrid Fredkin gate with quantum memories and single superconducting qubit in circuit QED and its applications, Opt. Express **26**, 4498 (2018).

[77] B. Ye, Z. F. Zheng, and C. P. Yang, Multiplex-controlled phase gate with qubits distributed in a multicavity system, Phys. Rev. A **97**, 062336 (2018).

[78] J. X. Han, J. L. Wu, Y. Wang, Y. Y. Jiang, Y. Xia, and J. Song, Multi-qubit phase gate on multiple resonators mediated by a superconducting bus, Opt. Express **28**, 1954 (2020).

[79] J. Majer, J. M. Chow, J. M. Gambetta, J. Koch, B. R. Johnson, J. A. Schreier, L. Frunzio, D. I. Schuster, A. A. Houck, A. Wallraff, A. Blais, M. H. Devoret, S. M. Girvin, and R. J. Schoelkopf, Coupling superconducting qubits via a cavity bus, Nature (London) **449**, 443 (2007).

[80] M. A. Sillanpää, J. I. Park, and R. W. Simmonds, Coherent quantum state storage and transfer between two phase qubits via a resonant cavity, Nature (London) **449**, 438 (2007).

[81] X. Li, Y. Ma, J. Han, Tao Chen, Y. Xu, W. Cai, H. Wang, Y. P. Song, Z. Y. Xue, Z. Q. Yin, and L. Sun, Perfect Quantum State Transfer in a Superconducting Qubit Chain with Parametrically Tunable Couplings, Phys. Rev. Appl. **10**, 054009 (2018).

[82] M. Hofheinz, E. M. Weig, M. Ansmann, R. C. Bialczak, E. Lucero, M. Neeley, A. D. O'Connell, H. Wang, J. M. Martinis, and A. N. Cleland, Generation of Fock states in a superconducting quantum circuit, Nature (London) **454**, 310 (2008).

[83] H. Wang, M. Mariantoni, R. C. Bialczak, M. Lenander, E. Lucero, M. Neeley, A. D. O'Connell, D. Sank, M. Weides, J. Wenner, T. Yamamoto, Y. Yin, J. Zhao, J. M. Martinis, and A. N. Cleland, Deterministic Entanglement of Photons in Two Superconducting Microwave Resonators, Phys. Rev. Lett. **106**, 060401 (2011).

[84] C. Wang, Y. Y. Gao, P. Reinhold, R. W. Heeres, N. Ofek, K. Chou, C. Axline, M. Reagor, J. Blumoff, K. M. Sliwa, L. Frunzio, S. M. Girvin, L. Jiang, M. Mirrahimi, M. H. Devoret, and R. J. Schoelkopf, A Schrödinger cat living in two boxes, Science **352**, 1087 (2016).

[85] Y. Xu, Y. Ma, W. Cai, X. Mu, W. Dai, W. Wang, L. Hu, X. Li, J. Han, H. Wang, Y. P. Song, Z. B. Yang, S. B. Zheng, and L. Sun, Demonstration of Controlled-Phase Gates between Two Error-Correctable Photonic Qubits, Phys. Rev. Lett. **124**, 120501 (2020).

[86] Y. Xu, J. Chu, J. Yuan, J. Qiu, Y. Zhou, L. Zhang, X. Tan, Y. Yu, S. Liu, J. Li, F. Yan, and D. Yu, High-Fidelity, High-Scalability Two-Qubit Gate Scheme for Superconducting Qubits, Phys. Rev. Lett. **125**, 240503 (2020).

[87] V. Negîrneac, H. Ali, N. Muthusubramanian, F. Battistel, R. Sagastizabal, M. S. Moreira, J. F. Marques, W. J. Vlothuizen, M. Beekman, C. Zachariadis, N. Haider, A. Bruno, and L. DiCarlo, High-Fidelity Controlled-Z Gate with Maximal Intermediate Leakage Operating at the Speed Limit in a Superconducting Quantum Processor, Phys. Rev. Lett. **126**, 220502 (2021).

[88] T. Abad, J. Fernández-Pendás, A. F. Kockum, and G. Johansson, Universal Fidelity Reduction of Quantum Operations from Weak Dissipation, Phys. Rev. Lett. **129**, 150504 (2022).

[89] J. R. Johansson, P. D. Nation, and F. Nori, QuTiP: An open source Python framework for the dynamics of open quantum systems, Comput. Phys. Commun. **183**, 1760 (2012).

[90] J. R. Johansson, P. D. Nation, and F. Nori, QuTiP 2: A Python framework for the dynamics of open quantum systems, Comput. Phys. Commun. **184**, 1234 (2013).

[91] M. Baur, S. Filipp, R. Bianchetti, J. M. Fink, M. Göppl, L. Steffen, P. J. Leek, A. Blais, and A. Wallraff, Measurement of Autler-Townes and Mollow Transitions in a Strongly Driven Superconducting Qubit, Phys. Rev. Lett. **102**, 243602 (2009).

[92] F. Yoshihara, Y. Nakamura, F. Yan, S. Gustavsson, J. Bylander, W. D. Oliver, and J. S. Tsai, Flux qubit noise spectroscopy using Rabi oscillations under strong driving conditions, Phys. Rev. B **89**, 020503(R) (2014).

[93] T. Niemczyk, F. Deppe, H. Huebl, E. P. Menzel, F. Hocke, M. J. Schwarz, J. J. Garcia-Ripoll, D. Zueco, T. Hümmer, E. Solano, A. Marx, and R. Gross, Circuit quantum electrodynamics in the ultrastrong-coupling regime, Nat. Phys. **6**, 772 (2010).

[94] F. Yan, S. Gustavsson, A. Kamal, J. Birenbaum, A. P. Sears, D. Hover, T. J. Gudmundsen, J. L. Yoder, T. P. Orlando, J. Clarke, A. J. Kerman, and W. D. Oliver, The flux qubit revisited to enhance coherence and reproducibility, Nat. Commun. **7**, 12964 (2016).

[95] J. Q. You, X. Hu, S. Ashhab, and F. Nori, Low-decoherence flux qubit, Phys. Rev. B **75**, 140515(R) (2007).

[96] A. Megrant, C. Neill, R. Barends, B. Chiaro, Y. Chen, L. Feigl, J. Kelly, E. Lucero, M. Mariantoni, P. J. J. O'Malley, D. Sank, A. Vainsencher, J. Wenner, T. C. White, Y. Yin, J. Zhao, C. J. Palmstrøm, J. M. Martinis, and A. N. Cleland, Planar superconducting resonators with internal quality factors above one million, Appl. Phys. Lett. **100**, 113510 (2012).

[97] W. Woods, G. Calusine, A. Melville, A. Sevi, E. Golden, D. K. Kim, D. Rosenberg, J. L. Yoder, and W. D. Oliver, Determining Interface Dielectric Losses in Superconducting Coplanar-Waveguide Resonators, Phys. Rev. Appl. **12**, 014012 (2019).